Reduced Coronal Emission above Large Isolated Sunspots

B. I. Ryabov, D. E. Gary, N. G. Peterova, K. Shibasaki, and N. A. Topchilo

Abstract We analyse specific regions of reduced soft X-ray and microwave emission in five large isolated sunspots. The *Nobeyama Radioheliograph* 17 GHz observations reveal a local depression of microwave brightness in the peripheral area of the sunspots. The depression regions appear light (weak absorption) in the He 10830 Å line in areas with extended ("open") field lines as indicated by potential field source surface model (PFSS) extrapolations up to 1.5 $R_{\odot}$. The observed depressions of 3 – 8% in ordinary mode at 17 GHz is interpreted as resulting from free-free emission under a decrease of 5 – 10% in plasma density. Our model estimates show that it is the decrement of density in both coronal and lower layers above the depression region that accounts for the depression. We believe that such depression regions are good candidates for marking the location of outward plasma motions.

Key words: Sun: corona, magnetic fields, radio emission

1. Introduction

Strong magnetic fields of solar active regions (ARs) confine plasma flows to be along field lines and thereby have influence on the temperature and density in distinct magnetic structures. Dark coronal areas in soft X-rays are caused by the lack of emitting material, that is, the shortage of density and/or temperature in the magnetic structures. Of special interest are the areas of reduced coronal emission where plasma outflows are expected.

B. I. Ryabov
Ventspils International Radio Astronomy Center, Inzhenieru st.101a, Ventspils LV-3601, Latvia
e-mail: ryabov@latnet.lv

D. E. Gary
Center for Solar-Terrestrial Research, New Jersey Institute of Technology, Newark, NJ 07102, USA
e-mail: dgary@njit.edu

N. G. Peterova
Special Astrophysical Observatory, St. Petersburg Branch, RAS, St. Petersburg, 196140, Russia
e-mail: peterova@yandex.ru

K. Shibasaki
e-mail: shibasaki.kiyoto@nao.ac.jp
Nobeyama Solar Radio Observatory, Nagano, 384-1305, Japan

N. A. Topchilo
V.V. Sobolev Astronomical Institute, St. Petersburg State University, 2 Bibliotechnaya Pl., Staryi Peterhoff, St.Petersburg, 198504, Russia
e-mail: topchilona@yandex.ru

Švestka *et al*. (1977) distinguished dark X-ray corridors in old ARs and small gaps in X-ray emission between the bright core of the AR and externally connected coronal loops. They noted the difficulty to distinguish between the cool large external loops and open field lines with rarefied plasma as the origin of the reduced coronal emission. The soft X-ray depletion just above sunspots has been examined by many authors (see e.g. Nindos *et al*., 2000 and references therein).

Other areas of reduced coronal emission are located in the region between shot, hot loops of bipolar ARs and the outer extended loops (Del Zanna, 2008). Doppler blue shifts in the EUV emission lines indicate plasma upflows at the peripheries of ARs (see Tian *et al*., 2010, for a review). Neupert *et al*. (1992) reported Doppler blue shifts in the line Mg IX (1.1×10^6 K) over the umbra of a large isolated sunspot. The authors argued that the region of the blue shift is the region of strong near-radial magnetic fields at both photospheric and coronal levels.

If there is a microwave counterpart of the reduced coronal emission, it might indicate the involvement of the lower layers of the atmosphere, or a distinct magnetic structure. It is of importance that microwave observations provide a means to derive plasma parameters.

Several cases of the local drop of intensity in sunspot-associated microwave sources have been reported to date. From observations with the *Westerbork Synthesis Radio Telescope* at 5 GHz Alissandrakis and Kundu (1982) reported the depression of intensity above the sunspot centre, which referred to the emission of cool plasma ($\sim 5\times10^5$ K).

Observations of large, isolated sunspots with a high angular resolution at cm wavelengths reveal notable details, especially in intensity of the ordinary mode. White, Kundu, and Gopalswamy (1991, 1992) reported a local drop by 3.5×10^3 K of the brightness temperature 1.5×10^4 K in ordinary mode from *Very Large Array* observations at 15 GHz. This reduced intensity referred to the lowest density in the atmosphere above the sunspot umbra.

Brosius and White (2004) analyzed coordinated observations of a large sunspot with the Very Large Array at 4.5, 8.0, and 14.6 GHz and three instruments aboard the *Solar and Heliospheric Observatory*. The authors concluded that the microwave emission from sunspot umbra is mainly due to a depressed gyroemission from the sunspot plume with cooler plasma.

Topchilo, Peterova, and Borisevich (2010) draw attention to the drop of intensity in ordinary mode over a large isolated sunspot. The brightness temperature dropped by $(1 - 2)\times10^3$ K below the brightness temperature of the quiet Sun in the frequency range 15.6 - 17 GHz. The third harmonic layer was suggested as the only effectively emitting layer in o-mode, which became transparent when the sunspot-associated source was near the central solar meridian.

Gary and Hurford (1987) discussed the shift of the position of sunspot associated sources toward the centre of a complex active region in both right and left circular polarizations at 16 frequencies in the range 1.4 – 8 GHz of the *Owens Valley Frequency-Agile Interferometer*. This shift persists at all heights involved and implies temperature and/or density deficit along field lines on the side of sunspots away from the centre of the active region.

In this paper we present the detection of the microwave counterpart of an area of reduced soft X-ray emission in five large, isolated sunspots. We discuss the influence of plasma parameters on the microwave emission in the depression region for both free-free and gyroresonance mechanisms. We find that only a decrease in plasma density can produce the observed microwave depression, consistent with the soft X-ray and He 10830 observations. Finally, we compare the observed depression at 17 GHz with a simulated decrease of plasma density using the model sunspot atmosphere of Obridko and Staude (1988), to estimate the extent of the reduction of density needed.

2. Observations

Our sample contains five large, isolated sunspots, selected due to their size and relative simplicity, and the availability of complementary data. The area of three of the sunspots is more than 300 millionths of the solar hemisphere, while two, AR 7529 and 7548, are slightly smaller. Each sunspot has no appreciable neighbouring sunspots within a radius of 7 heliographic degrees. This means rather an applied than a strict definition of an isolated sunspot. The sunspots of AR 7417 and AR 11289 have two umbrae within one penumbra. We confine our study to times when the ARs are close to the solar disc centre in order to reduce projection effects.

The microwave sources associated with the large isolated sunspots (Table 1) were analysed using 17 GHz maps in both right (*R*) and left (*L*) circular polarization. The *Nobeyama Radioheliograph* (NoRH) provides Stokes *I* and *V* maps of the Sun at 17 GHz with an angular resolution 18″. Following Koshiishi (2003), we adopted total intensity $I = 10^4$ K as the intensity of the quiet Sun at 17 GHz. The quiet Sun level is defined to be 10^4 K in right and left circular polarization as well.

Bezrukov *et al*. (2011) and Bezrukov, Ryabov, and Shibasaki (2012) converted *I* and *V* maps to $R = I + V$ and $L = I - V$ maps in their study of the depressed 17 GHz emission. In the NoRH database *I* and *V* maps were routinely produced with dissimilar CLEAN parameters in the image reconstruction process. Hence, recalculating *R* and *L* in this way is not entirely correct. To avoid this problem, in this paper, *R* and *L* maps are synthesized and cleaned independently using identical parameters.

The predominance of extraordinary (x-) mode over ordinary (o-) mode emission in stable sunspot-associated microwave sources was shown by Zlotnik (1968) using model simulations and is well confirmed observationally. Hence, we take the brightness temperature in the extraordinary (x-) mode T_B^x as the observed intensity of the dominant polarization, *R* or *L* according to the N or S magnetic polarity of the sunspot. The degree of circular polarization is calculated as $P = (T_B^x - T_B^o)(T_B^x + T_B^o)^{-1}$. In the T_B^x and T_B^o contour maps of Figures 1, 3 – 6 the contour levels are in steps of 10^3 K starting from 9×10^3 K to 1.5×10^4 K and in steps of 2×10^4 K starting from 2×10^4 K. A downhill line indicates contours of 9×10^3 K and 10^4 K.

Table 1 The extrema of 17 GHz intensities in the normal modes observed with the *Nobeyama Radioheliograph* for the observed active regions.

AR	Date of CMP		17 GHz brightness temperatures at maximum T_B^x		17 GHz brightness temperatures at minimum T_B^o			
		θ [a] [degree]	maxT_B^x [10^3 K]	T_B^o [10^3 K]	minT_B^o [10^3 K]	T_B^x [10^3 K]	r [b] [arcsec]	B_{max} [c] [G]
7417	1993 Feb. 8.3	-1.7	265.0	14.4	8.0	8.4	13.9	2400S
7529	1993 June 29.3	0.9	91.2	18.7	9.3	9.5	2.7	2400N
10105	2002 Sep. 13.6	-8.8	188.1	13.9	8.7	8.8	7.1	3100S
10743	2005 Mar. 15.7	-7.2	45.3	13.0	9.0	9.1	14.0	2900S
11289	2011 Sep. 13.6	10.2	225.6	24.4	8.5	8.7	5.9	3600S

[a] The longitudinal distance of the sunspot from the central solar meridian in the NoRH image.

[b] r denotes the distance between the maximal longitudinal magnetic field B_l and the maximal T_B^x at 17 GHz.
[c] The strength and polarity of the sunspot magnetic field according to Crimean Astrophysical Observatory. S (south) and N (north) correspond to negative and positive polarity, respectively.

We will later use the radio scans of AR 11289 obtained with the RATAN-600 radio telescope to illustrate the effect of reduced emission in o-mode at high frequencies. The telescope produces a fan beam with the narrow dimension of 18.1", 18.45", and 20.13" at the frequencies 15.78 GHz, 15.45 GHz, and 14.14 GHz, respectively.

We will also compare the Nobeyama images with images in the chromospheric absorption line He 10830 Å, taken from the National Solar Observatory, Kitt Peak (NSO/KP) and from the Mauna Loa Solar Observatory (MLSO; see Elmore *et al*., 1998). The light area (weak absorption) in 10830 Å images imply a low plasma density in the upper coronal layers, which accounts for the reduced soft X-ray emission available for the excitation of the line. The typical dimension of the weak absorption is ~ 100"– 200". According to Brajša *et al*. (1996) the He I images show weak absorption in coronal holes and strong absorption in active regions. Hence, the light area within sunspots is of special interest.

To estimate the shift of the peak of x-mode intensity from the peak magnetic field, we will use longitudinal magnetograms from the National Solar Observatory, *Kitt Peak* (NSO/KP) *magnetograph* (ARs 7417, 7529, and 10105), the *Solar and Heliospheric Observatory, Michelson Doppler Imager* (SOHO/MDI) (AR 10743), and the *Solar Dynamics Observatory, Helioseismic and Magnetic Imager* (SDO/HMI) (AR 11289).

The following subsections provide the comparison of the specific feature of locally concave contours of 17 GHz intensity (which signal a depression of radio emission) with the corresponding 10830 Å image, soft X-ray image, or with the footpoints of extrapolated magnetic field lines. The accuracy of the image overlay is estimated to be 5". As the reference time for co-registration was the time of the NoRH image, the NSO/KP, *Yohkoh Soft X-ray Telescope* (*Yohkoh*/SXT) images, and magnetograms were corrected for solar rotation to correspond to that time.

2.1. Active region 7417

The area of the locally reduced (dark) soft X-ray and 17 GHz (locally concave contours) emission, as well as weak absorption in 10830 Å are located to the north of the two umbrae (Figure 1). The arrow points at this area of the size 20" – 40". Hereafter we refer to such areas as the "depression region" in 17 GHz maps.

The brightness temperature of the sunspot source in x-mode, T_B^x, ranges from 1.3×10^4 K at the western border of the sunspot-associated source to the maximal value of 2.65×10^5 K near the centre of the eastern umbra. (The borders of umbrae and penumbrae correspond to 11 February. In fact, there were two umbrae within one penumbra of the AR 7417 on 8 February).

The brightness temperature in o-mode varies over a range of a few thousand Kelvin $T_B^o = (1.1 - 1.6)\times10^4$ K. The extreme degree of circular polarization P = 90% is found at the maximum of T_B^x.

The locations of the minimal brightness temperatures in both modes nearly coincide. The region of local depression is extended in nearly the same direction as the general growth of T_B^o in the AR: from minimal T_B^o to the area spanned by hot and dense coronal loops. The region of the local depression occurs on the side of the sunspot-associated source of reduced soft X-ray and microwave intensity. However, there are high brightness temperatures T_B^x in the core of the sunspot source, which conceal the local depression. As a result, ΔT_B^x is perceptible in the peripheral area of the source yet too small to be measured with confidence.

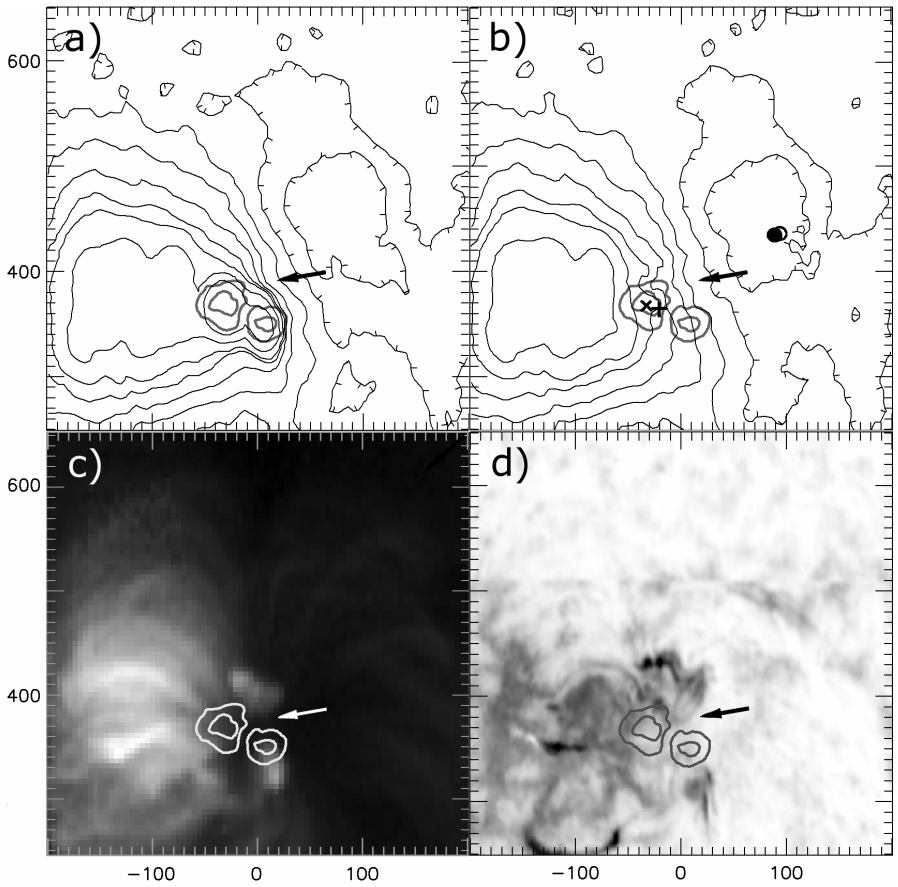

Figure 1 AR 7417 observed on 8 February 1993. (a) T_B^x and (b) T_B^o contour maps of 17 GHz NoRH images (02:52 UT). Here and in later figures the levels are at 0.9, 1, (downhill line), 1.1, 1.2, 1.3, 1.4, 1.5, 2, 4×10^4 K (solid line). (c) Soft X-ray image (*Yohkoh*/SXT; 02:48 UT). (d) He I 10830 Å image (NSO/KP; 19:04 UT on 7 February). Hereafter the meaning of the symbols in (b) are: ○ - minimum T_B^x, ● - minimum T_B^o, x - maximum T_B^x at 17 GHz, + - maximum of the strength of the longitudinal magnetic field. The axis units are in seconds of arc from the centre of the solar disc; solar north is up, solar west is to the right. Here the location of minimum T_B^o nearly coincides with that of minimum T_B^x.

The depression at 17 GHz is estimated referring to the interpolation line (the dashed line of the cubic spline in Figure 2) which represents the undepressed section of the contour of interest (the bold line of 1.4×10^4 K contour) in the depression region. The spline goes through a set of undepressed points of the contour. The depression at the chosen point A (dot) on the interpolation line is the difference of the brightness temperatures of the contour of interest and the other depressed contour, which is tangent to or intersects the point A. Hence, the local depression $\Delta T_B^o = 1.4\times10^4$ K - 1.31×10^4 K = 900 K is relative to the undepressed background of $T_B^o = 1.4\times10^4$ K at the point A.

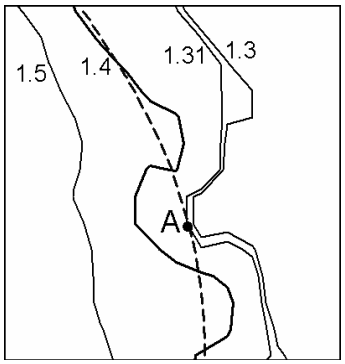

Figure 2 Sketch of the depression region to illustrate the determination of the depression ΔT_B^o in the AR 7417. The cubic spline (dashed line) represents the undepressed section of the contour T_B^o = 1.4×10^4 K (bold line). The contour 1.31×10^4 K intersects the chosen point A (dot) on the spline and indicates the difference between the depressed and undepressed brightness temperatures at the point A.

The measured shift between the location of the maximum of longitudinal field B_l and maximum T_B^x is r = 13.9" (Table 1). The time delay of ~ 11 hours between the NoRH and the NSO/KP observations (7 February, 15:28; Figure 8a) might introduce uncertainty into the shift.

2.2. Active region 7529

T_B^x ranges from 1.3×10^4 K at the southern border of the sunspot source to the maximal value of 9.2×10^4 K near the centre of the umbra. Note the change of T_B^x contours into concentric in the core of the sunspot source, indicating a local depression of T_B^x in the depression region (Figure 3a).

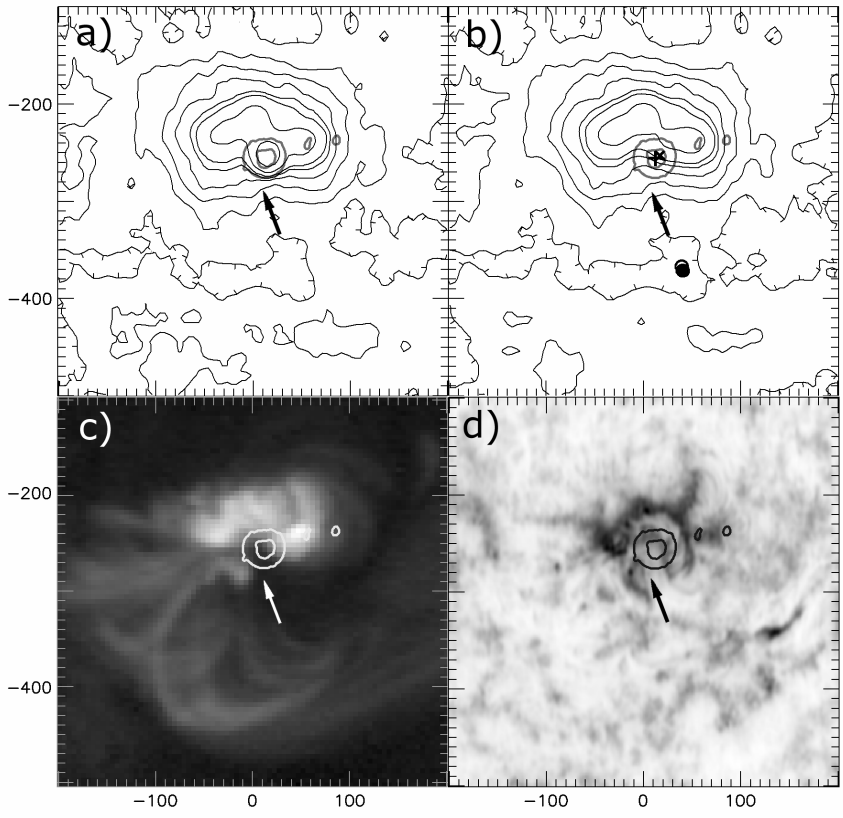

Figure 3 AR 7529 observed on 29 June 1993. (a) T_B^x and (b) T_B^o contour maps of 17 GHz NoRH images (02:53 UT). (c) Soft X-ray image (*Yohkoh*/SXT; 01:46 UT). (d) He I 10830 Å image (NSO/KP; 16:06 UT).

The brightness temperature in o-mode ranges $T_B^o = (1.3 – 2.1)\times10^4$ K. The maximum degree of polarization P = 69% is found near the maximum T_B^x. The maximum depression of $\Delta T_B^o = 590$ K ($P = 8\%$) is relative to the background $T_B^o = 1.3\times10^4$ K.

2.3. Active region 10105

Panels c in Figures 3 and 4 show extrapolated magnetic field lines overlaid on corresponding SOHO/MDI magnetograms. The field lines are extrapolated by means of the potential-field source-surface model (PFSS) up to the altitude of 1.5 $R_\odot$. Nitta and DeRosa (2008) noted that the PFSS extrapolations reproduce reliable open magnetic fields for coronal holes but may not show open field lines for active regions.

T_B^x ranges from 1.3×10^4 K to 1.88×10^5 K near the centre of the western sunspot. The maximum degree of polarization $P = 86\%$ is collocated with the maximum of T_B^x. The depression $\Delta T_B^x = 800$ K is relative to a background of $T_B^x = 1.3\times10^4$ K (X = -194″, Y = -263″). It is noteworthy that the depression region is clearly seen in x-mode in this case since it is outside the gyro resonance core of the microwave source.

The brightness temperature in o-mode, T_B^o, ranges over $(1.3 – 1.5)\times10^4$ K. The maximum depression in o-mode $\Delta T_B^o = 1100$ K (P = 1.5%) is relative to the background value $T_B^o = 1.3\times10^4$ (X = -190″, Y = -259″). Another location within the depression region (X = -210″, Y = -270″; Table 2) is more remote from the sunspot.

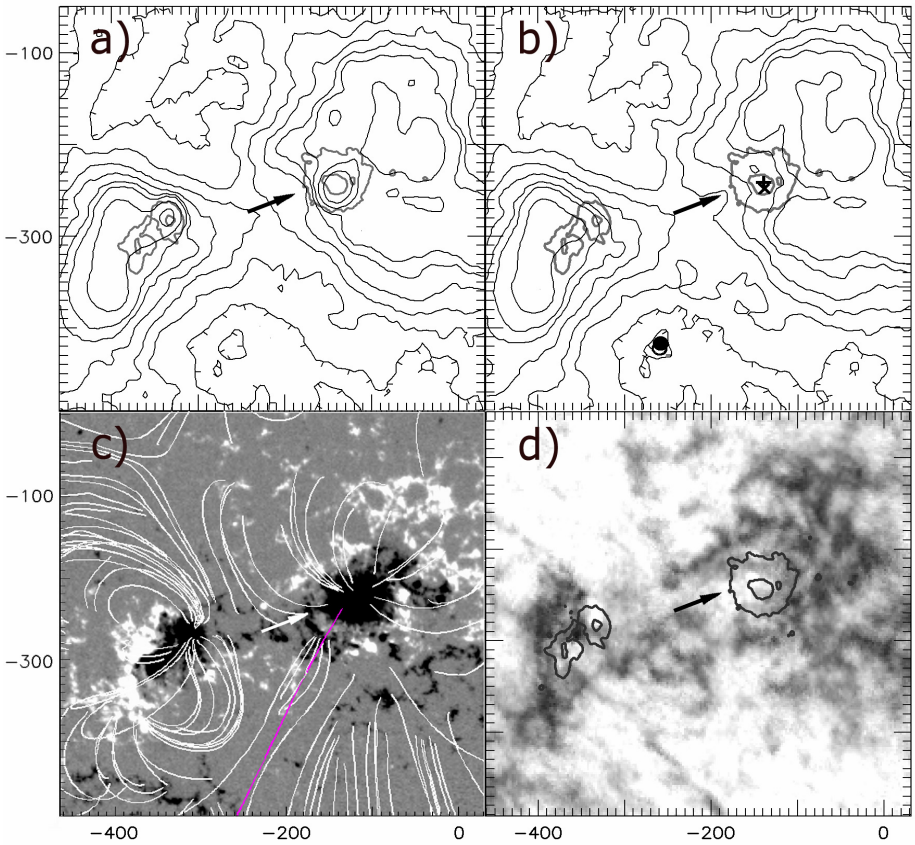

Figure 4 AR 10105 observed on 13 September 2002. (a) T_B^x and (b) T_B^o contour maps of 17 GHz NoRH images (02:45 UT). (c) The magnetic field lines extrapolated with the potential field source

surface model (courtesy of Lockheed Martin Solar and Astrophysics Laboratory (LMSAL); 04:47). The arrow points at the footpoint of an open field line. (d) He I 10830 Å image (Mauna Loa Solar Observatory, CHIP; 16:59 UT).

Topchilo, Peterova, and Borisevich (2010) revealed from the RATAN-600 observations of the AR 10105 that the intensity depression in o-mode appeared at frequencies from 16.4 down to 12.95 GHz with no depression at frequencies ≤ 11.25 GHz. Furthermore, they showed that the circular polarization drops from $P \sim 100\%$ at 12.95 GHz to 20% at 11.25 GHz. Note that the magnetic field strength of 2000 G corresponds both to the magnetic field of the 3rd harmonic of gyro frequency f_B, at the observing frequency $f_{17} = 3f_B \approx 17$ GHz, and to the 2nd harmonic of the observing frequency $f_{11} = 2f_B \approx 2/3 \times 17$ GHz ≈ 11.3 GHz. In other words, if intense x-mode emission comes from the 3rd harmonic layer at 17 GHz, one might expect that the o-mode brightness of the 2nd harmonic layer at 11.3 GHz is high enough to contribute, thus reducing the circular polarization at frequencies ≤ 11.3 GHz.

2.4. Active region 10743

The brightness temperature T_B^x ranges from 1.2×10^4 K at the northwest border of the sunspot source to the maximal value of 4.5×10^4 K near the southern border of the sunspot umbra. The intensity in o-mode ranges within $T_B^o = (1.1 - 1.38) \times 10^4$ K. The maximum degree of circular polarization $P = 55\%$ is located at the maximum of T_B^x. The maximum depression $\Delta T_B^o = 400$ K ($P = 30\%$) is relative to the background $T_B^o = 1.3 \times 10^4$ K. The depression in x-mode is negligibly small (below the noise level of the image).

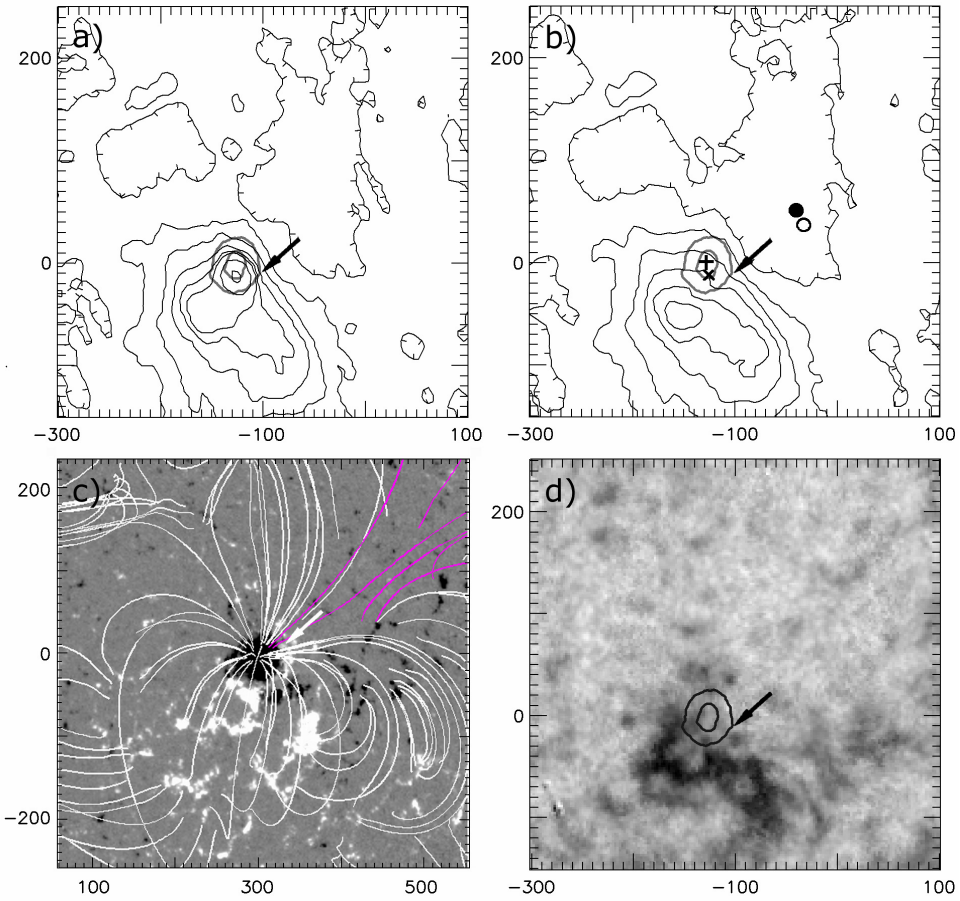

Figure 5 AR 10743 observed on 15 March 2005. (a) T_B^x and (b) T_B^o contour maps of 17 GHz NoRH images (02:45 UT). (c) The magnetic field lines extrapolated with the potential field source surface

model (courtesy of LMSAL; 17 March 03:15). The arrow points at the footpoint of an open field line. (d) He I 10830 Å image (Mauna Loa Solar Observatory, CHIP; 19:11 UT).

Note that the image of the magnetic field lines extrapolated with the PFSS (Figure 5c) is presented for a time two days later than the time of the NoRH contour maps.

The bright region ~ 200" in the north-west direction from the sunspot (Figure 5d), and its extension toward the sunspot, is the feature we wish to highlight for comparison.

2.5. Active region 11289

The brightness temperature T_B^x across the sunspot source ranges from 1.3×10^4 K at the northern border of the source to the maximal value of 2.25×10^5 K in the southern umbra. The intensity in o-mode ranges within $T_B^o = (1.2 - 3.5)\times10^4$ K. The maximum degree of polarization P = 81% is found near the maximum of T_B^x. There is no apparent local depression region in either o- or x-mode at 17 GHz. One might perceive wide concavity of the contour 1.2×10^4 K in both normal modes at 17 GHz.

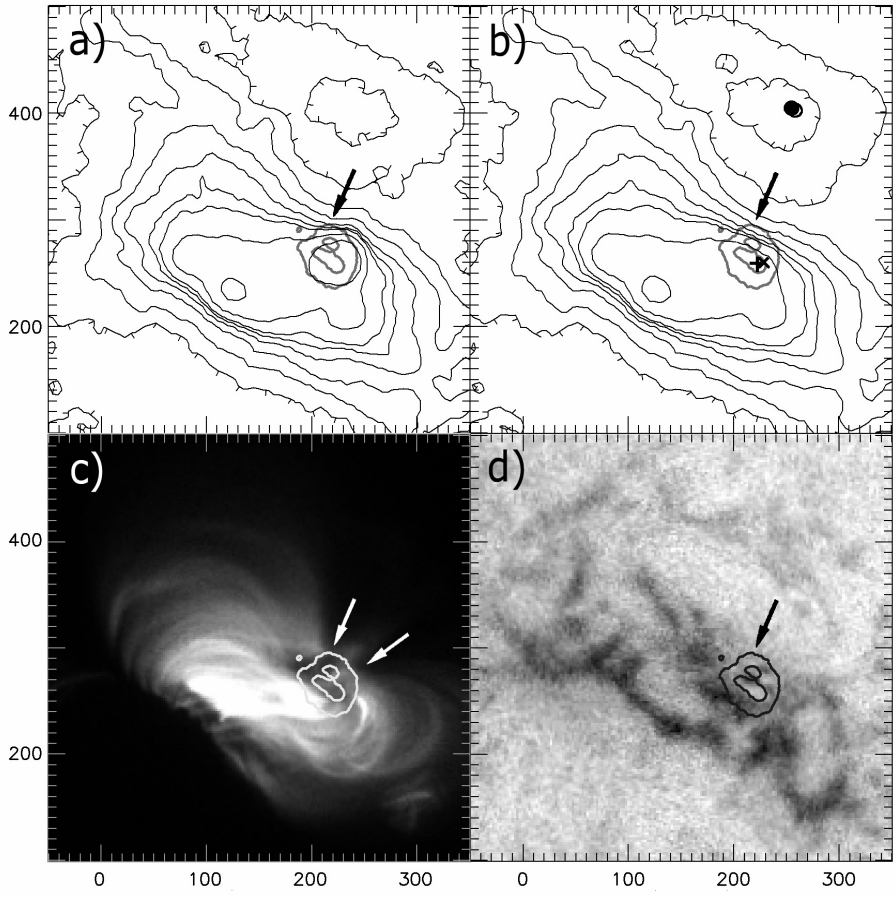

Figure 6 AR 11289 observed on 14 September 2011. (a) T_B^x and (b) T_B^o contour maps of 17 GHz NoRH images (02:55 UT). (c) Soft X-ray image (*Hinode, X-Ray Telescope (*XRT*)*; 10:04 UT). (d) He I 10830 Å image (Mauna Loa Solar Observatory, CHIP; 13 September 18:45 UT).

The depression in o-mode is clearly seen in the 1D scan observed with the RATAN-600 telescope at the observing frequencies of 14.14 – 15.78 GHz (Figure 7). Taking into account the direction of the scan, we concluded that the depression region occurs over the western area of the sunspot source. The additional arrow on Figure 6c marks a second locally reduced soft X-ray brightness of this area. The ratio of the depressed (western) and less depressed

(eastern) radio flux in o-mode varies as follows: 1 at 15.75 GHz, 0.5 at 15.45 GHz, and 0.08 at 14.15 GHz.

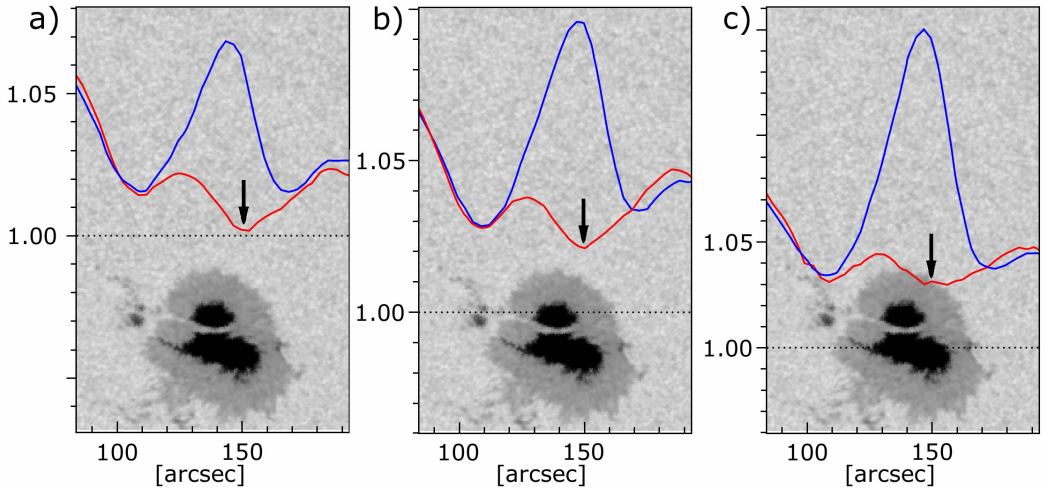

Figure 7 AR 11289 observed on 14 September 2011. The radio scan in the o- (red line) and x-mode (blue line) observed with the RATAN-600 radio telescope (09:09 UT) at the frequencies (a) 15.75 GHz, (b) 15.45 GHz, and (c) 14.15 GHz is overlaid on a white light image (SDO/HMI; 09:15 UT). The microwave intensity is in units relative to the quiet Sun level (dotted line).

3. Results and Discussions

The main observational result of this paper is the correspondence between the location of the depressed 17 GHz emission in o-mode and the location of the reduced soft X-ray emission in the atmosphere of the large isolated sunspots. Close inspection showed the absence of any cool Hα filament in the depression regions that might have absorbed microwaves in the depressed region.

In this Section we discuss the influence of plasma parameters on the microwave emission in the depression region. To compare the relative contribution of the parameters we cite the opacity formulae for both free-free and gyroresonance mechanisms. Then we discuss which parameter can produce the dominant effect on the depression, consistent with the soft X-ray and He 10830 observations. Finally, we compare the observed depression at 17 GHz with that simulated as a decrease of plasma density within the model sunspot atmosphere of Obridko and Staude (1988).

3.1. Opacity formulae

The microwaves from the sunspot atmosphere can be described in terms of the ordinary (o) and extraordinary (x) normal waves due to the free-free and gyroresonance mechanisms of radiation. The polarization of the waves in the solar atmosphere is circular with opposite senses. The plasma parameters, electron temperature T, density N, magnetic field B, and propagation angle α enter the opacity formulae for the free-free and the gyroresonance radiation.

For the case of quasi-longitudinal propagation, the free-free optical thickness of the isothermal layer with the longitudinal component of magnetic field $B_l = |B \cos \alpha|$ depends on the plasma parameters in the form (Zheleznyakov, 1970):

$$\tau_{ff}^{o,x} \propto \xi\, T^{1.5}\, EM\, (f \pm f_B\, |\cos \alpha|\,)^{-2} = \xi\, T^{1.5}\, EM\, (f \pm 2.8{\times}10^6\, B_l)^{-2}, \qquad (1)$$

where f is the observing frequency, the emission measure EM is integrated squared density along the ray path $EM = \int N^2 \, dl$, ξ is a slowly varying function of N and T, and f_B is the gyro frequency $f_B = eB/(2\pi m_e c)$. All units are in cgs. If the component B_l becomes stronger, the opacity for the o-mode wave decreases, but the opacity for the x-mode wave increases (sign "-" in the denominator).

Zheleznyakov (1970) gave the gyroresonance optical thickness averaged over the line profile of the gyroresonance layer as:

$$\tau_{g\text{-}r}^{o,x} \propto T^{s-1} N f^{1} F^{o,x}(\alpha,s), \qquad (2)$$

where $F^{o,x}(\alpha,s)$ are two functions which depend strongly on the propagation angle α. Equation (2) is valid for the case of low plasma density $N[cm^{-3}] << 1.2\times10^{-8} f^2[Hz^2]$, α away from 90°, and harmonic numbers of the gyroresonance layer s = 2, 3, 4. Viewing along the magnetic field lines $\alpha \rightarrow 0$ the gyroresonance layers become transparent $F^{o,x}(\alpha,s) \rightarrow 0$. For a given α and s, $F^{o}(\alpha,s)$ is about two orders of magnitude lower than $F^{x}(\alpha,s)$.

At observing frequency $f = 1.7\times10^{10}$ Hz, the gyroresonance layers correspond to the strengths of magnetic field 3040 G (s = 2), 2030 G (s = 3), and 1520 G (s = 4). By means of model simulations Vourlidas, Gary, and Shibasaki (2006) established that the harmonic layer s = 3 could be optically thick at 17 GHz in x-mode for a wide range of the plasma parameters. Photospheric sunspot fields stronger than 2200 G are needed in order to raise the s = 3 layer in x-mode to the height of transition region temperatures and produce observable intensity. Nindos *et al*. (2000) found that in order to account for the high circular polarization P = 70 – 90% observed when sunspot sources are near the CMP, the layer s = 2 must have essentially no contribution to the o-mode intensity at 17 GHz.

The ratio of the optical thicknesses $\tau_{g\text{-}r}^{o,x}/\tau_{ff}^{o,x}$ is proportional to $T^{s+0.5} N^{-1}$, which demonstrates the relative contribution of the radiation mechanisms to brightness temperature under the same values of T and N. The gyroresonance radiation is favoured by high T and low N whereas the free-free radiation is favoured by low T and high N.

3.2. Magnetic fields

Extreme magnetic fields can produce the local depression of the microwave emission in sunspot-associated source near the CMP.

According to Equation (1), strong B_l results in a small optical thickness in o-mode τ_{ff}^{o}. Then the free-free emission in o-mode comes from the lower and colder layers of the atmosphere. However, it is not the case that strong B_l underlies the depression regions on the periphery of the sources (except AR 10743; Table 2). The concave contours on T_B^{o} maps tend to appear between the ridges of the magnetic peaks.

The weak magnetic fields produce the low-lying gyroresonance layers and therefore low brightness temperatures of the gyroresonance emission. In Subsection 3.4 we accept the free-free radiation as the sole origin of the 17 GHz intensity in o-mode on the periphery of the sunspot source near the CMP. The only non-peripheral depression region in o-mode seems to span over the sunspot of the AR 10105. There are no indications of weak magnetic fields over the centre of the sunspot in the direction indicated by arrow on Figure 8c. On the contrary, the gyroresonance emission in x-mode provides high polarization P = 86% and fills the depression in x-mode in the core of the source (Figure 4a).

We conclude that the depression in the peripheral area of the 17 GHz sources is not due to the variation of magnetic field strength. However, it seems to be related to the change of magnetic connectivity, since the microwave depressions appear at locations where the field

line connectivity has a large gradient (quasi-separatrix layers). Baker *et al*. (2009) has shown that the plasma outflows are co-spatial with the location of quasi-separatrix layers.

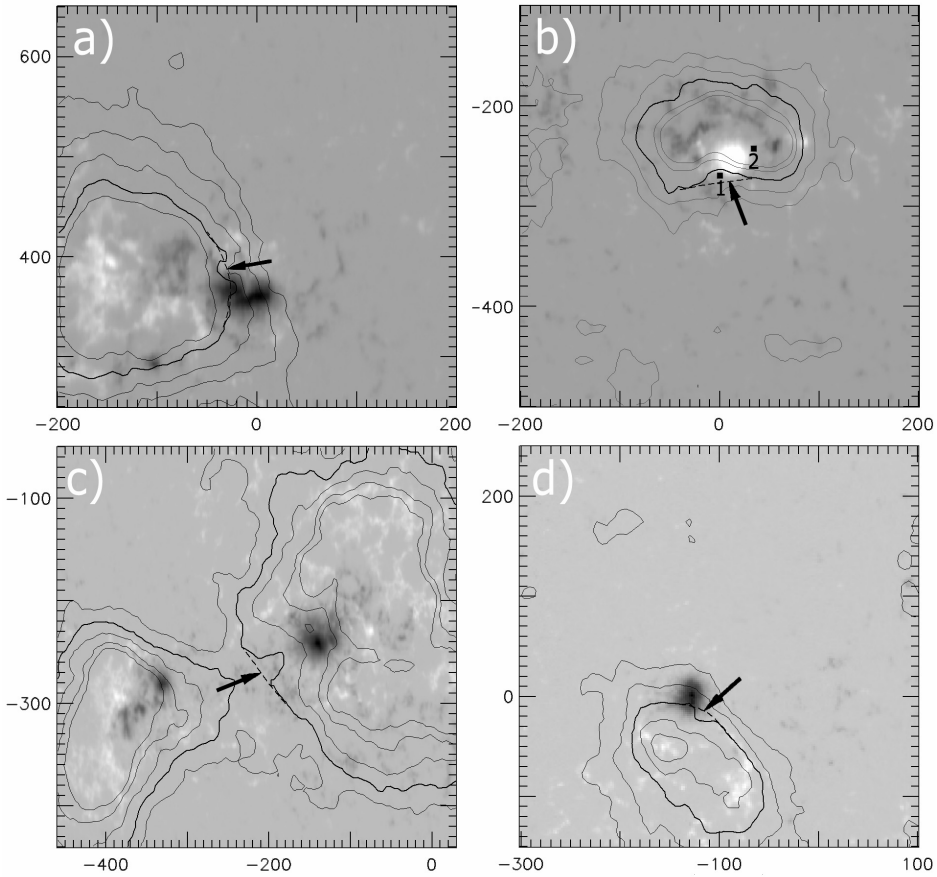

Figure 8 $T_B{}^o$ contour maps of 17 GHz NoRH images. The contours (11, 12, 13, 14, 15)×10^3 K overlaid on the longitudinal magnetograms. The contour of reference (thick line) is as follows (a) 14×10^3 K in AR 7417, (b) 13×10^3 K in AR 7529, (c) 12×10^3 K in AR 10105, and (d) 13×10^3 K in AR 10743. The arrows point to the reference locations (X, Y) in Table 2. In the AR 7529 (Panel b) the photospheric field B_l = 85 G is the same in both locations 1 and 2 (see Subsection 3.3).

Table 2 Depression regions observed with the *Nobeyama Radioheliograph* at 17 GHz.

AR	Time	$\Delta T_B{}^o$ [10^2 K]	$T_B{}^o$ [10^3 K]	X [arcsec]	Y [arcsec]	B_l [a] [G]
7417	1993 Feb. 8.12	9.0	14	-30	388	0
7529	1993 June 29.12	5.9	13	10	-275	20N
10105	2002 Sep. 13.11	3.2	12	-210	-270	20S
10743	2005 Mar. 15.11	4.0	13	-115	-15	600S

[a] The longitudinal magnetic field B_l is interpolated to the reference location (X, Y) using corresponding longitudinal magnetogram referred to in Section 2.

3.3. The electron temperature and density

To evaluate the role of temperature and density on the depression at 17 GHz let us examine the coronal contribution of free-free emission in two locations with equal strengths of longitudinal magnetic fields.

Nindos *et al*. (2000) presented the measurements of the coronal temperature and emission measure above isolated sunspots. The distributions show positive correlation between the reduced soft X-ray emission and low values of the coronal emission measure of this emission.

We adopted the measurements across the sunspot AR 7529 on 29 June 1993. The profile of the *EM* and *T* comes along the line between the locations 1 and 2 (Figure 8b). This profile showed the lowest value of the EM while crossing the depression region at the location 1.

We chose a comparison location 2 at which the longitudinal component of the photospheric magnetic field is the same as in location 1, *i.e.* $B_{l2} = B_{l1} = 85$ G at both locations. The NoRH brightness temperatures are as follows: $T_B^x = 1.62\times10^4$ K, $T_B^o = 1.27\times10^4$ K at $X_1 = 1''$, $Y_1 = -269''$ and $T_B^x = 2.4\times10^4$ K, $T_B^o = 2.17\times10^4$ K at $X_2 = 33''$, $Y_2 = -242''$. Since the degree of polarization, $P_1 = 12\%$ and $P_2 = 5\%$, is low near the outer borders of the sunspot penumbra, we suggest that 17 GHz emission is due to free-free radiation in these locations.

The coronal temperature and emission measure (in units of cm^{-5}) found from soft X-rays in the two locations are (following Nindos *et al*., 2000): $T_1 = 1.7\times10^6$ K, $T_2 = 5.3\times10^6$ K, log $EM_1 = 26.5$ and log $EM_2 = 28.1$. The optically thin coronal layers at $f = 17$ GHz add to brightness temperature due to free-free emission: $T_B^{o,x} \approx \tau_{ff}^{o,x}\, T \approx 0.27\, T^{-0.5}\, EM\, (f \pm 2.8\times10^6\, B_l)^{-2}$. The ratio of coronal increments from the above two locations is proportional to $T_{B2}/T_{B1} \propto (T_2/T_1)^{-0.5}\, (EM_2/EM_1) = 0.566\times39.8 = 22.5$. We see that *the low emission measure is the major factor* that affects the brightness temperature at the peripheral area of the sunspot source and, hence, on the local depression. The ratio of the coronal densities in the two locations is $(EM_2/EM_1)^{0.5} \approx 6$, assuming equal lengths of *EM* integration in the two coronal regions of soft X-ray emission.

Analysing soft X-ray images and PFSS extrapolations, Arge *et al*. (2003) revealed narrow dark features ("narrow coronal holes") in soft X-ray images. The narrow coronal holes may extend into ARs and occur above relatively strong magnetic fields $B > 100$ G. However, the depression regions presented here are not of great length and are not confied to areas of predominantly one magnetic polarity, although there is low-density coronal plasma and extended ("open") field lines in several depression regions. The corresponding areas of reduced soft X-ray emission above the depression regions do not expand into extended features over a period of several solar rotations. We conclude that the depression regions are not identified with narrow coronal holes.

3.4. The model estimates of plasma density

To have a notion of the plasma densities needed to account for the observed depression at 17 GHz, we simulated the free-free and gyroresonance emission in the model atmosphere of the sunspot umbra given by Obridko and Staude (1988). The simulation was done for the entire microwave sunspot-associated source to improve comparability. Here we analyse mainly the 17 GHz brightness temperature in o-mode T_B^o in terms of density variation in the atmosphere of the sunspot when it is near the CMP.

The expressions for the absorption coefficients of free-free and gyroresonance radiation were taken from Zlotnik (1968). The calculation procedure was reported by Peterova and Ryabov (1981). The sunspot field is extrapolated assuming a simple dipole submerged 2.16×10^9 cm beneath the level of photosphere, which provided the maximum photospheric strength of 3000 G.

We confirm the findings of the work by Vourlidas, Gary, and Shibasaki (2006), where simulations were carried out under the same model atmosphere and model magnetic fields. Namely, (1) the gyroresonance emission at 17 GHz arises from 3rd gyroresonance layer; (2) $P > 30\%$ is a relevant polarization criterion to discriminate the highly polarized gyroresonance emission from free-free emission. Our model simulations determine the area-discrimination of the radiation mechanisms for the 17 GHz sunspot source near the CMP. Namely, the gyroresonance emission in x-mode (s = 3 layer) prevails in the core of the sunspot source

while the free-free emission prevails on the periphery of the sunspot source in the intensity of both o- and x-mode.

Let us summarize the characteristic values to analyze. The direction of increasing T_B^o across the observed sunspot sources is close to the line joining the reduced coronal emission in the soft X-rays to the other side of the source spanned by hot and dense coronal loops (Figures 1, 3, and 6). The observed brightness temperatures T_B^o range from $(1.1 – 1.4)\times10^4$ K on the side of minimal intensity to $(1.3 – 3)\times10^4$ K on the opposite side on the periphery of the sunspot sources. Our simulations lead to somewhat higher brightness temperatures of $T_B^o = (2.1 – 2.2)\times10^4$ K, indicating that an adjustment to the model is needed.

To fit T_B^o to the observed background of the depression region, that is $(1.1 – 1.4)\times10^4$ K, one needs to decrease not only the coronal density but also the density of lower layers. As noted by Nindos *et al*. (2000), the coronal contribution to the brightness temperature at 17 GHz is of only 170 – 600 K within the source. Therefore we reduced the model densities by the correction factor k_N in all the outer layers $z \geq 1.18\times10^8$ cm ($T > 7000$ K, $N < 2.57\times10^{10}$ cm^{-3}). Actually, we do not know the precise atmospheric structure of a region with such rarefied plasma. Hence, our model estimates in terms of the plasma density height distribution are tentative and meant for illustration only.

The correction factor $k_N = 0.16$ resulted in simulated $T_B^o = (1.2 – 1.3)\times10^4$ K over the sunspot source. Under a further reduction to $k_N = 0.15$ the brightness temperature T_B^o was diminished by $\Delta T_B^o = 500$ K. Hence, a decrease in model density by 6% at $z \geq 1.18\times10^8$ cm can provide the required depression at 17 GHz. The observed background of T_B^o was thus provided by plasma density $1/0.16 \approx 6$ times more rarefied than in the model atmosphere introduced by Obridko and Staude (1988). For example, the model density 1.4×10^9 cm^{-3} at altitude $z = 3\times10^8$ cm drops to $N = 2.25\times10^8$ cm^{-3} under $k_N = 0.16$ and $N = 2.11\times10^8$ cm^{-3} under $k_N = 0.15$.

The model simulations also show that the semitransparent x-mode gyroresonance layer s = 3 is located at altitudes up to $z = 3\times10^8$ cm, where $T = 1.17\times10^6$ K. The simulated brightness temperature varies from $T_B^x = 2.6\times10^5$ K under $k_N = 1$ to $T_B^x = 6\times10^4$ K under $k_N = 0.16$. The gyroresonance radiation does not contribute noticeably to T_B^o over the core of the sunspot source which is near the solar disc centre.

The intensity of free-free emission grows with the increasing distance from the CMP due to the growing length of the ray-path and growing contribution from hotter layers. The gyroresonance emission grows due to the gyroresonance layer s = 3 which becomes more opaque at 17 GHz with distance from the CMP. Thus, the deepest depression is expected at the time of the CMP.

4. Summary and Conclusions

The presented NoRH observations at 17 GHz have provided us the opportunity to study the brightness temperatures with confidence, since *R*- and *L*-maps were synthesized and cleaned independently using the same parameters. On the basis of these observations, we identified small regions of depressed 17 GHz emission in o-mode in the peripheral area of the large isolated sunspots. The location of the depression region corresponds to the location of reduced soft X-ray emission and relatively weak absorption in the He 10830 Å line. The PFSS extrapolations provide evidence for the presence of high magnetic gradient in field line connectivities, including extended (“open”) magnetic field lines over the depression region in three of five sunspots.

The conclusions are as follows:

1. We can estimate some plasma parameters from already known radiation mechanisms in two separate parts of the 17 GHz source, which is associated with a large isolated sunspot. When the source is near the CMP the dominant radiation mechanism might differ by area: (a) in the peripheral area, the free-free radiation contributes to the intensity in o-mode, (b) in the core of the source, the 3rd gyroresonance layer contributes to the intensity in x-mode.
2. The 20" – 40"-size region of local depression at 17 GHz appears on the side of the sunspot source with reduced microwave and soft X-ray emission. This region of 3 – 8% depressed intensity in o-mode holds plasma of 5 – 10% lower density than in the adjacent regions of the sunspot atmosphere. With reference to the altitude 3×10^8 cm and temperature 1.17×10^6 K of the sunspot model atmosphere by Obridko and Staude (1988) the estimated coronal density is 2×10^8 cm^{-3}.
3. The revealed depression regions are not the active-region coronal holes. The depression regions do not overlie areas of predominantly one magnetic polarity and do not expand into extended features over a period of several solar rotations.

In our view, the sunspot atmosphere above the depression regions is a candidate for the source of outward plasma flow. The further tests of Doppler shifts in the EUV emission lines over the depression regions in the large isolated sunspots will prove our suggestion. The presented finding of the depression region could lead to more sophisticated models of physical conditions, including the specified plasma flows and the height profile of the extended field lines.

Acknowledgements This work was supported by the Latvian Council of sciences in the frame of the project Nr. 11.1856. DG is supported by NSF grants AGS-09059761, AST-1312802, AGS-1250374, and NASA grant NNX11AB49G to NJIT. NT is supported by SPbSU grant 6.0.26.2010. BR appreciates the hospitality and help of the Nobeyama Solar group during his stay at the Nobeyama Radio Observatory. We are grateful to the National Solar Observatory, Kitt Peak, the Mauna Loa Solar Observatory, the Debrecen Heliophysical Observatory and the Nobeyama Radio Observatory teams for making their data available. This work was partly carried out on the Solar Data Analysis System operated by the Astronomy Data Center in cooperation with the Hinode Science Center of the National Astronomical Observatory of Japan. We thank the anonymous referee for the useful comments that helped improve the manuscript. We are grateful to Kazumasa Iwai and Dmitry Bezrukov for the assistance in preparing the data and the model estimates.

References

Alissandrakis, C.E., Kundu, M.R.: 1982, *Astrophys. J.* **253**, L49. doi: 10.1086/183734.

Arge, C.N., Harvey, K.L., Hudson, H.S., Kahler, S.W.: 2003, *Proceedings of the Tenth International Solar Wind Conference.* AIP Conference Proceedings **679**, 202. doi: 10.1063/1.1618577.

Baker, D., van Driel-Gesztelyi, L., Mandrini, C.H., Démoulin, P., Murray, M.J.: 2009, *Astrophys. J.* **705**, 926. doi: 10.1088/0004-637X/705/1/926.

Bezrukov, D., Ryabov, B., Peterova, N., Topchilo, N.: 2011, *Latvian Journal of Physics and Technical Sciences* **48***,* 2, 56. doi: 10.2478/v10047-011-0016-7.

Bezrukov, D. A., Ryabov, B. I., Shibasaki, K.: 2012, *Baltic Astronomy* **21**, 509.

Brajša R., Pohjolainen S., Ruždjak V., Sakurai T., Urpo S., Vršnak B., Wöhl H.: 1996, *Solar Phys.* **163**, 1, 79-91. doi: 10.1007/BF00165457.

Brosius, J.W., White, S.M.: 2004, *Astrophys. J.* **601**, 546. doi: 10.1086/380394.

Del Zanna, G.: 2008, *Astron. Astrophys.* **481**, L49. doi: 10.1051/0004-6361:20079087.

Elmore, D. F., Card, G. L., Chambellan, C.W., Hassler, D. M., Hull, H. L., Lecinski, A. R., MacQueen, R. M., Streander, K. V., Streete, J. L., White, O. R.: 1998, *Applied Optics* **37**, 19, 4270. doi: 10.1364/AO.37.004270.
Gary, D.E., Hurford, G.J.:1987, *Astrophys. J.* **317**, 522. doi: 10.1086/165296.
Koshiishi, H.: 2003, *Astron. Astrophys* **412**, 893. doi: 10.1051/0004-6361:20031514.
Neupert, W.M., Brosius, J.W., Thomas, R.J., Thompson, W.T.: 1992, *Astrophys. J.* **392**, L95. doi: 10.1086/186434.
Nindos, A., Kundu, M.R., White, S.M., Shibasaki, K., Gopalswamy, N.: 2000, *Astrophys. J.* **130**, 485. doi: 10.1086/317355.
Nitta, N.V., DeRosa, M.L.: 2008, *Astrophys. J.* **673**, L207. doi: 10.1086/527548.
Obridko, V. N., Staude, J.: 1988, *Astron. Astrophys.* **189**, 232.
Peterova, N.G., Ryabov, B.I.: 1981, *Soviet Astron*. **25**, 609.
Švestka, Z., Solodina, C.V., Howard, R., Levin, R.H.: 1977, *Solar Phys.* **55**, 2, 359. doi: 10.1007/BF00152579.
Tian, H., Marsch, E., Tu, C., Curdt, W., He, J.: 2010, *New Astronomy Reviews* **54**, 13. doi: 10.1016/j.newar.2010.08.001.
Topchilo, N.A., Peterova, N.G., Borisevich, T.P.: 2010, *Astronomy Reports* **54**, 69. doi: 10.1134/S1063772910010087.
Vourlidas A., Gary D.E., Shibasaki K.: 2006, *Pub. Astron. Soc. Japan* **58**, 11. doi: 10.1093/pasj/58.1.11.
White, S.M., Kundu, M.R., Gopalswamy, N.: 1991, *Astrophys. J.* **366**, L43. doi: 10.1086/185905.
White, S.M., Kundu, M.R., Gopalswamy, N.:1992, *Astrophys. J. Suppl. Ser.* **78**, 599. doi: 10.1086/191641.
Zlotnik, E.Ya.: 1968, *Soviet Astronomy* **12**, 245.
Zheleznyakov, V.V.: 1970, *Radio Emission of the Sun and Planets*, Oxford, Pergamon Press.

Figure captions

Figure 1 AR 7417 observed on 8 February 1993. (a) T_B^x and (b) T_B^o contour maps of 17 GHz NoRH images (02:52 UT). Here and in later figures the levels are at 0.9, 1, (downhill line), 1.1, 1.2, 1.3, 1.4, 1.5, 2, 4×10^4 K (solid line). (c) Soft X-ray image (*Yohkoh*/SXT; 02:48 UT). (d) He I 10830 Å image (NSO/KP; 19:04 UT on 7 February). Hereafter the meaning of the symbols in (b) are: ○ - minimum T_B^x, ● - minimum T_B^o, x - maximum T_B^x at 17 GHz, + - maximum of the strength of the longitudinal magnetic field. The axis units are in seconds of arc from the centre of the solar disc; solar north is up, solar west is to the right. Here the location of minimum T_B^o nearly coincides with that of minimum T_B^x.

Figure 2 Sketch of the depression region to illustrate the determination of the depression ΔT_B^o in the AR 7417. The cubic spline (dashed line) represents the undepressed section of the contour $T_B^o = 1.4\times10^4$ K (bold line). The contour 1.31×10^4 K intersects the chosen point A (dot) on the spline and indicates the difference between the depressed and undepressed brightness temperatures at the point A.

Figure 3 AR 7529 observed on 29 June 1993. (a) T_B^x and (b) T_B^o contour maps of 17 GHz NoRH images (02:53 UT). (c) Soft X-ray image (*Yohkoh*/SXT; 01:46 UT). (d) He I 10830 Å image (NSO/KP; 16:06 UT).

Figure 4 AR 10105 observed on 13 September 2002. (a) T_B^x and (b) T_B^o contour maps of 17 GHz NoRH images (02:45 UT). (c) The magnetic field lines extrapolated with the potential field source surface model (courtesy of Lockheed Martin Solar and Astrophysics Laboratory (LMSAL); 04:47). The arrow points at the footpoint of an open field line. (d) He I 10830 Å image (Mauna Loa Solar Observatory, CHIP; 16:59 UT).

Figure 5 AR 10743 observed on 15 March 2005. (a) T_B^x and (b) T_B^o contour maps of 17 GHz NoRH images (02:45 UT). (c) The magnetic field lines extrapolated with the potential field source surface model (courtesy of LMSAL; 17 March 03:15). The arrow points at the footpoint of an open field line. (d) He I 10830 Å image (Mauna Loa Solar Observatory, CHIP; 19:11 UT).

Figure 6 AR 11289 observed on 14 September 2011. (a) T_B^x and (b) T_B^o contour maps of 17 GHz NoRH images (02:55 UT). (c) Soft X-ray image (*Hinode, X-Ray Telescope (*XRT*)*; 10:04 UT). (d) He I 10830 Å image (Mauna Loa Solar Observatory, CHIP; 13 September 18:45 UT).

Figure 7 AR 11289 observed on 14 September 2011. The radio scan in the o- (red line) and x-mode (blue line) observed with the RATAN-600 radio telescope (09:09 UT) at the frequencies (a) 15.75 GHz, (b) 15.45 GHz, and (c) 14.15 GHz is overlaid on a white light image (SDO/HMI; 09:15 UT). The microwave intensity is in units relative to the quiet Sun level (dotted line).

Figure 8 T_B^o contour maps of 17 GHz NoRH images. The contours (11, 12, 13, 14, 15)$\times10^3$ K overlaid on the longitudinal magnetograms. The contour of reference (thick line) is as follows (a) 14×10^3 K in AR 7417, (b) 13×10^3 K in AR 7529, (c) 12×10^3 K in AR 10105, and (d) 13×10^3 K in AR 10743. The arrows point to the reference locations (X, Y) in Table 2. In the AR 7529 (Panel b) the photospheric field $B_l = 85$ G is the same in both locations 1 and 2 (see Subsection 3.3).